



This is a repository copy of *Analysis of a high temperature reciprocating hammer type impact wear apparatus*.

White Rose Research Online URL for this paper:

<https://eprints.whiterose.ac.uk/222590/>

Version: Accepted Version

---

**Article:**

Shabana, M., Tomlinson, K. [orcid.org/0000-0003-4691-5057](https://orcid.org/0000-0003-4691-5057) and Slatter, T. (2025) Analysis of a high temperature reciprocating hammer type impact wear apparatus. *Wear*. 205814. ISSN 0043-1648

<https://doi.org/10.1016/j.wear.2025.205814>

---

© 2025 The Authors. Except as otherwise noted, this author-accepted version of a journal article published in *Wear* is made available via the University of Sheffield Research Publications and Copyright Policy under the terms of the Creative Commons Attribution 4.0 International License (CC-BY 4.0), which permits unrestricted use, distribution and reproduction in any medium, provided the original work is properly cited. To view a copy of this licence, visit <http://creativecommons.org/licenses/by/4.0/>

**Reuse**

This article is distributed under the terms of the Creative Commons Attribution (CC BY) licence. This licence allows you to distribute, remix, tweak, and build upon the work, even commercially, as long as you credit the authors for the original work. More information and the full terms of the licence here:

<https://creativecommons.org/licenses/>

**Takedown**

If you consider content in White Rose Research Online to be in breach of UK law, please notify us by emailing [eprints@whiterose.ac.uk](mailto:eprints@whiterose.ac.uk) including the URL of the record and the reason for the withdrawal request.



[eprints@whiterose.ac.uk](mailto:eprints@whiterose.ac.uk)  
<https://eprints.whiterose.ac.uk/>

# 25th International Conference on Wear of Materials

## Analysis of a High Temperature Reciprocating Hammer Type Impact Wear Apparatus

--Manuscript Draft--

<b>Manuscript Number:</b>	WOM2024-D-24-00134R1
<b>Article Type:</b>	SI: Wear of Materials 2025
<b>Keywords:</b>	impact wear; High temperature; Stainless steel; Inconel
<b>Corresponding Author:</b>	Tom Slatter, PhD, MEng Loughborough University Loughborough, UNITED KINGDOM
<b>First Author:</b>	Muaad Shabana, MEng
<b>Order of Authors:</b>	Muaad Shabana, MEng Katherine Tomlinson, BSc, PhD Tom Slatter, PhD, MEng
<b>Abstract:</b>	<p>Impact wear can occur when objects collide repeatedly causing damage to the surface of one or both objects. The underlying mechanisms that result in material loss, or displacement, from the contact are primarily surface fatigue and plastic deformation. Adhesion, abrasion and oxidative wear also can occur depending on the contact geometry, the operating conditions, and environment. Temperature is a key parameter and, depending on the application, can accelerate the mechanisms that are dominant at lower temperatures or cause other mechanisms to increasingly contribute, often synergistically. This is particularly the case in applications, for example in the energy, process and aerospace industries, where complex mechanisms that translate and rotate large loads operate at temperatures at or exceeding the thermal limits of the materials they are necessarily made from.</p> <p>There are a number of reciprocating hammer type impact apparatus described in literature that can be used for fundamental investigations, but none are capable of achieving the necessary temperatures in the contact zone of between 600°C and 1250°C, indeed many solely operate at room temperature. As a consequence, there is little information about the mechanistic role of temperature in impact wear.</p> <p>This work, therefore proposes a new high temperature impact wear test rig, initially capable of running reciprocating impact wear tests at temperatures up to 750 °C. The design process and features are described before presenting the results of impact wear tests conducted using specimens manufactured from an austenitic chromium-nickel stainless steel (AISI 304) and a nickel-based superalloy (Inconel 625). The tests ranged from room temperature to 750 °C, rising in increments of 250 °C. Stainless steel experienced a greater wear rate with increasing temperatures, whilst the superalloy experienced a reduced wear rate with increasing temperatures. Reflections on the use of the apparatus are also offered to inform others of suggested best practice.</p>

1  
2  
3  
4  
5  
6  
7  
8  
9  
10  
11  
12  
13  
14  
15  
16  
17  
18  
19  
20  
21  
22  
23  
24  
25  
26  
27  
28  
29  
30  
31  
32  
33  
34  
35  
36  
37  
38  
39  
40  
41  
42  
43  
44  
45  
46  
47  
48  
49  
50  
51  
52  
53  
54  
55  
56  
57  
58  
59  
60  
61  
62  
63  
64  
65

- Analysis of a reciprocating hammer type impact wear apparatus capable of conducting testing at up to 750°C
- Provides a protocol, or suggested best practice, to guide users of similar apparatus to enable easier comparison of experimental data for tests conducted at high temperatures.
- Gives initial insight into the high temperature impact wear resistance of AISI 304 stainless steel and Inconel 625.

# Analysis of a High Temperature Reciprocating Hammer Type Impact Wear Apparatus

Shabana, M.<sup>a</sup>, Tomlinson, K.,<sup>a</sup> and Slatter, T.<sup>a,b</sup>

<sup>a</sup> The Leonardo Tribology Centre, School of Mechanical, Aerospace and Civil Engineering, The University of Sheffield, Mappin Street, Sheffield, U.K. S1 3JD

<sup>b</sup> The Wolfson School of Mechanical, Electrical & Manufacturing Engineering, Loughborough University, Epinal Way, Loughborough, Leicestershire, U.K. LE11 3TU

\* corresponding author: t.j.slatter@lboro.ac.uk

## Abstract

Impact wear can occur when objects collide repeatedly causing damage to the surface of one or both objects. The underlying mechanisms that result in material loss, or displacement, from the contact are primarily surface fatigue and plastic deformation. Adhesion, abrasion and oxidative wear also can occur depending on the contact geometry, the operating conditions, and environment. Temperature is a key parameter and, depending on the application, can accelerate the mechanisms that are dominant at lower temperatures or cause other mechanisms to increasingly contribute, often synergistically. This is particularly the case in applications, for example in the energy, process and aerospace industries, where complex mechanisms that translate and rotate large loads operate at temperatures at or exceeding the thermal limits of the materials they are necessarily made from.

There are a number of reciprocating hammer type impact apparatus described in literature that can be used for fundamental investigations, but none are capable of achieving the necessary temperatures in the contact zone of between 600°C and 1250°C, indeed many solely operate at room temperature. As a consequence, there is little information about the mechanistic role of temperature in impact wear.

This work, therefore proposes a new high temperature impact wear test rig, initially capable of running reciprocating impact wear tests at temperatures up to 750 °C. The design process and features are described before presenting the results of impact wear tests conducted using specimens manufactured from an austenitic chromium-nickel stainless steel (AISI 304) and a nickel-based superalloy (Inconel 625). The tests ranged from room temperature to 750 °C, rising in increments of 250 °C. Stainless steel experienced a greater wear rate with increasing temperatures, whilst the superalloy experienced a reduced wear rate with increasing temperatures. Reflections on the use of the apparatus are also offered to inform others of suggested best practice.

**Keywords:** impact wear, high temperature, stainless steel, Inconel

# 1 Introduction

Impact wear can be defined as damage to a surface due to repetitive contact by another body. This can cause damage to machining tools or lead to development of larger cracks that cause component failure [1]. It occurs in many applications; however, it causes the most significant damage to gas turbines, combustion engines, machining tools, construction equipment, and mining equipment [2], [3], [4], [5], [6]. In those cases, impact wear may lead to shorter component lifetime or lower efficiency during operation. Therefore, it is of interest to study and understand impact wear to be able to optimise part performance and maintenance.

The main factors affecting how much a material wears are: “design, applied load, contact area and degree of movement, lubrication, environment, and material properties (surface finish, hardness and steel microstructure)” [7]. These factors are often intertwined, as some materials may experience hot hardness, reducing the level of wear at high temperatures [8]. This study will focus on changing the material properties and environment (temperature) to determine their direct influence on impact wear. Impact wear may be normal or compound in nature, as shown in Figure 1. In compound impacts, both impact and sliding wear occur simultaneously which produces different types of impact scars [9].

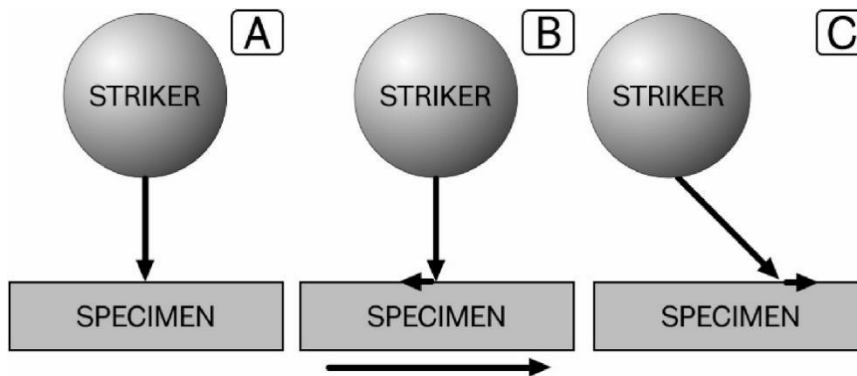


Figure 1 - Diagram showing different modes of impact wear [9]

With the exception of those designed for solely testing specific components, test apparatus for testing the fundamental nature of impact wear predominantly operate at room temperature, with some with the potential to go up to 350-400 °C. This temperature is much lower than the temperatures experienced in gas turbines, heat exchangers and similar large scale thermofluids industrial devices, some of which are systems that experience the highest levels of impact wear [2]. Gas turbines, for example can operate at temperatures between 600 °C and 1250 °C [10] and impact wear occurs in a number of different mechanisms, damage to which can impair the control of the combustion process thus reducing efficiency and causing higher fuel consumption [11]. To be able to accurately predict materials performance at such high temperatures, testing must be done near this range, especially where the operating temperature nears or exceeds material properties such as hot hardness.

Impact wear tests are carried out to measure how a specimen is affected by impact wear in various loading conditions. These tests are vital in understanding how a material/component will wear during its lifetime. Studies have also been done to create models for predicting wear rates for impact wear [12], [13]. Lewis et al. concluded that experimental data is required to make models more accurate [13]. This highlights the importance of extensive testing to develop an accurate understanding of wear. It also indicates that the most accurate method of predicting impact wear is by conducting experiments. Slatter et al. showed the range of different results that

can be obtained by changing just the material [14]. Different materials exhibit different scar widths, scar depths, scar shapes due to the multiple wear mechanisms involved with impact, previously stated by others to be oxidation, adhesion, abrasion, surface fatigue and plastic deformation [1].

Impact wear at high temperatures has not been extensively studied, with only two studies in the literature dedicated to pure impact wear at high temperature [15], [16]. Recently, Chen et al. conducted testing between 25 °C to 450 °C. Volume loss was then used to characterise the wear rate. For 2.25Cr–1Mo steel, wear volume increased at 225 °C then decreased at 450 °C but remained higher than 25 °C. The main wear mechanisms were delamination, plastic deformation, and oxidative wear. Delamination was dominant at 225 °C, while plastic deformation was dominant at 450 °C. In the mid-1990s, Ootani et al. conducted impact wear and impact-sliding wear tests at room temperature, 200 °C and 400 °C [16]. This study tested SUH36 steel rings and Fe-base sintered alloy disks together, then compared the wear in both. Impact-sliding wear shows an overall similar trend to that found by Chen et al. In this case wear volume is highest at 200 °C, then 400 °C, then room temperature. It is important to note that this similarity may be caused by similarities in the materials tested. As the wear remains highly material dependent. Ootani et al. found that the materials were softest at 200 °C, which may explain the higher wear rate. While at 400 °C oxidation occurred which led to the increase in wear compared to room temperature, but kept it limited. These studies show the importance of conducting testing on specific materials as each material will react differently to high temperatures and pure impact wear. Also, the highest temperature reached in these papers is only 450 °C, significantly below the operating temperatures experienced by some engineering materials when in use.

There is some research considering wear at high temperatures, but these mainly focus on sliding wear and impact-abrasive (rather than impact hammering as here) wear mechanisms [17], [18], [19], [20]. Varga et al. conducted testing on two materials. Material A is a “Ni-based alloy with tungsten carbide reinforcement” and Material B “carbide rich Fe-based complex alloy”. They showed that wear at room temperature could not be directly correlated to wear at high temperature within the same material, but high temperature hot hardness reduced wear in one material. This led to the finding that a stable microstructure at high temperature is a better indicator of wear performance than hardness [17]. Hernandez et al. tested adhesive and abrasive wear using a sliding wear mechanism. Wear rates for boron steels and ferritic alloys were measured. Both materials exhibited the same wear rate at room temperature. However, wear rate for boron steel decreased with temperature, while it increased with temperature for ferritic steels. This indicates that tougher materials exhibit better wear performance at higher temperatures.

On the other hand, papers by Kesavan et al. and Zhou et al. showed a clearer correlation between higher temperatures and increased wear resistance. Kesavan et al. tested 316 stainless-steel with wear resistant coating at 300 °C and 550 °C. Different wear mechanisms dominated at different temperatures, with an overall improvement in wear resistance at higher temperatures [19]. Zhou et al. conducted testing at 20 °C, 100 °C, 200 °C and 400 °C. Wear volume initially increased at 100 °C, then reduced at higher temperatures. The second lowest temperature tested by Kesavan et al. was higher than the corresponding temperature in any of the literature reviewed. This may explain the linear improvement of wear resistance with increased temperatures, as the metal’s behaviour between room temperature and 300 °C was not characterised and suggests that the interpolation of the results by Kesavan et al. may have led to an inaccurate conclusion.

This also highlights the importance of conducting testing at various temperatures to ensure the behaviour of the material is comprehensively understood.

It has been shown that hardness within the elastic regime is one of the main factors influencing impact wear [12] where softer materials exhibit more wear, plastic flow, and smooth wear scar edges. While harder materials exhibit less wear, rougher wear scar edges, and evidence of brittle fracture starting [14]. Hardness alone is not a sufficient indicator of wear, as it has been shown that hard brittle materials may experience more wear [18]. Therefore it is important to consider a material's toughness and elasticity to form realistic predictions of its wear resistance [12], [18].

Temperature has a significant impact on metal properties. Temperature can affect a metal's mechanical properties, electrical conductivity, magnetic behaviour, and corrosion resistance. This is all due to the atomic interactions within the metal [21]. These changes may be positive or negative depending on the metal alloy and heating method employed [22], [23]. Hardness significantly decreases with temperature for austenitic alloys, for example. Another important change at high temperatures is oxidation occurring, with a general trend in metals of high temperatures leading to higher oxidation rates. This can act as a protective layer to metals which reduces the level of wear experienced [24]. Oxidation is often cited as a potential reason for the improved wear rate at high temperatures [15], [16], [18], [20]. The exact rate and impact of oxidation will be dependent on each material.

It can be seen that different metal alloys will have significantly different wear rates and scars under the same conditions. Hardness has a significant influence when it comes to wear rates, and it may vary with temperature. It has been demonstrated the variety of results that may come from wear testing at high temperatures. It showed that there is a gap in impact wear testing at high temperatures, with the temperatures above 450 °C being omitted. It is of importance to conduct impact wear testing up to 750 °C, to address the gap in the research and develop the understanding of how metal alloys will wear in high temperature applications.

The aim of the work presented, therefore, is to further develop and improve the general concept of the apparatus described by Slatter et al. [14] into a new design of apparatus that is capable of testing at significantly higher temperatures than other designs available in literature and overcomes the limitations of the previous design, particularly the 'hidden' impacts resulting from the striker's motion being uncontrolled in certain modes of operation.

It should be noted that, for clarity and readability, throughout this work the apparatus described by Slatter et al. [14] that this follows on from will be variously described as 'the previous apparatus', 'the previous design', or similar.

## **2 Experimental Methodology**

### **2.1 Design**

A schematic of the general apparatus concept, layout and motion can be seen in Figure 2. A 3 kW electric motor rotates the camshaft thus providing the required reciprocating motion to the striking hammer, via the pivoting arm. A limitation of a previous design of this type of apparatus [14] was that excessive rotational speed of the cam would result in the motion of the arm being uncontrolled. In the apparatus developed here, the hammer is more controlled by means of a different design of cam and an improved arrangement of arm-spring-cam (maintaining the utility of the spring lightly loading the arm against to game) rather than simply relying on acceleration due to gravity. The end of the arm that contacts the cam has a replaceable follower-type sleeve

made from a laminate phenolic resin composite bearing material to minimise wear and to facilitate easy replacement when wear has eventually occurred. The counterface specimens are similar to those used before, being (nominally) 35mm diameter, 10mm thick discs and 10mm diameter AISI 51200 steel balls as strikers. The designs for the sample holders are shown in Figure 3.

The sample holders are enclosed in an insulated chamber containing half-cylinder Fibrothal® heating elements with a nominal rated power of 650W each (Figure 4). To reduce the heating power requirements and minimise the use of specialist high temperature alloys, the chamber size was made as compact as possible with as much of the apparatus as possible being outside of the chamber. This was achieved in part by using stainless steel housings, incorporating all the heating elements and insulation, connected and hinged together in a clamshell-like configuration (Figure 4). This ensures that the heating modules experience no force from the hammer and allows for both sides of the furnace to be opened for ease of access to the sample holders. The design is capable of achieving temperatures in excess of 750 °C

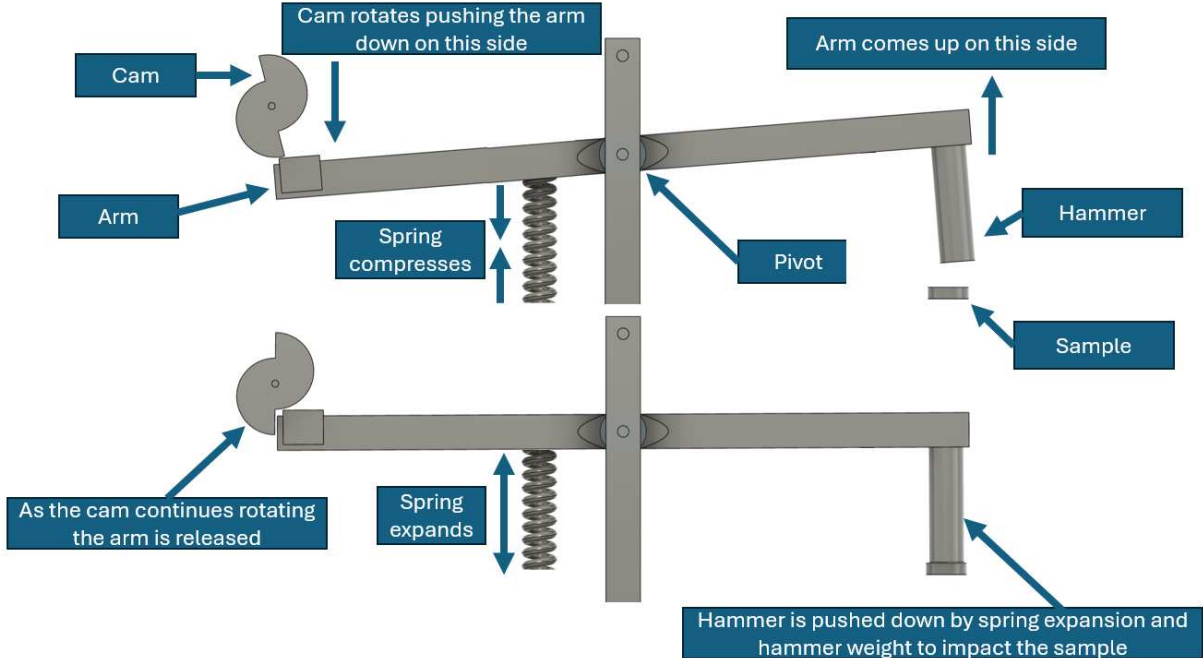


Figure 2 - Simplified side view diagram of general layout and concept of operation.

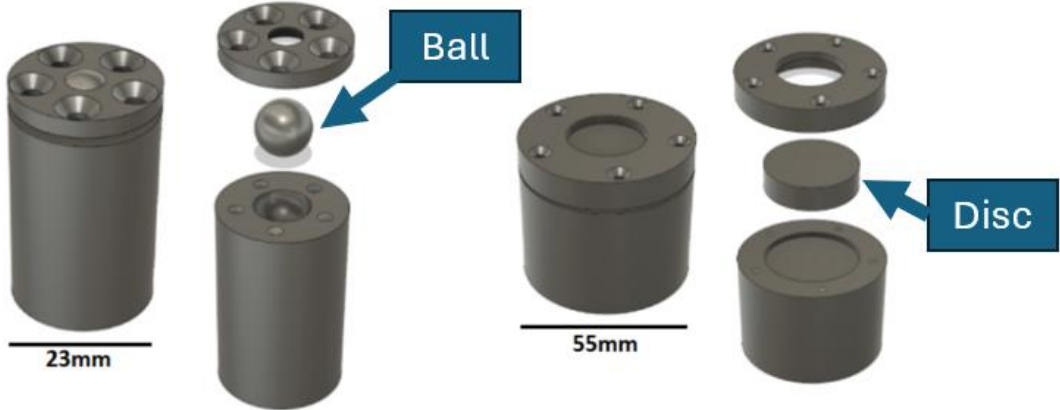


Figure 3 - Exploded hammer (left) and sample holder (right) design.



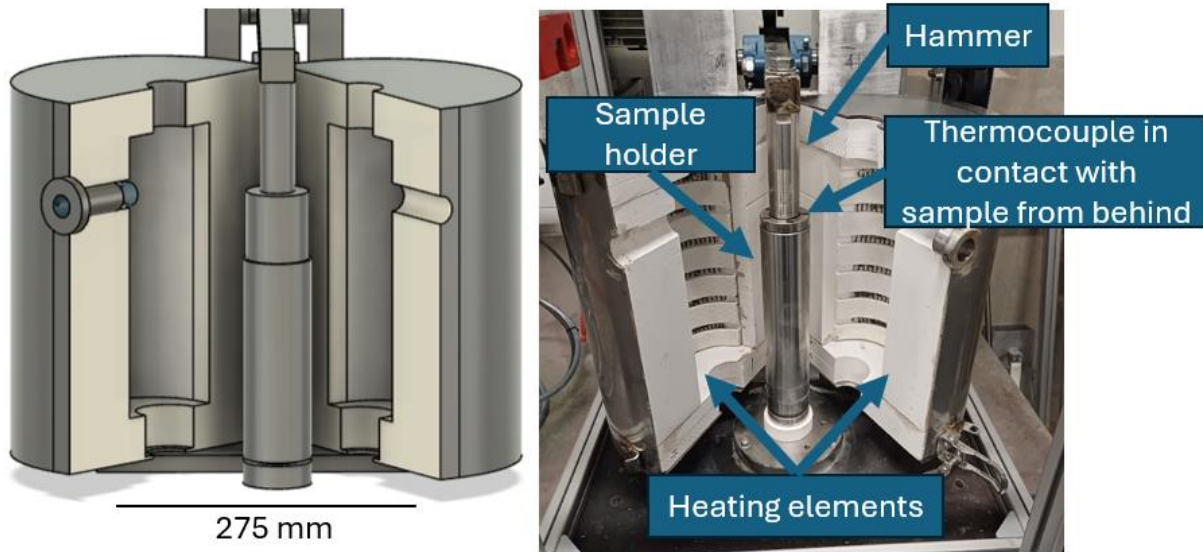


Figure 4 - New furnace shell design; CAD (left), as manufactured (right).

## 2.2 Assumptions

To allow comparison with the previous apparatus, similar assumptions and constraints were made during the design:

- The pivoting arm and the components driving it, other than the controlling spring, are perfectly stiff so deflections and vibrations related to the operation of the apparatus can be ignored. It is also assumed that the entire apparatus is on a perfectly stiff mass that is much larger than the mass of the moving components.
- The inertia of the arm and striker is ignored so as to assume that the cam is in contact with the arm throughout the rotation of the cam.
- That the arm and cam remain in contact throughout each cycle at a given operating frequency.
- That the resulting striker-specimen contact is 'normal' (Figure 1, type A) as the striker is spherical and the arc length (and corresponding small angle) the striker travels is small.

In the previous analysis these first three assumptions were shown to be a significant source of error due to the uncontrolled motion of the arm and resulting 'hidden' impacts.

- The motion resulting from the shape of the cam is identical to that described by the design and for all tests. This will change as materials wear, potentially changing the mechanics, but is unlikely to be of significance (assuming the wear is monitored and components changed as required).

- The temperature of the specimen remains constant and accurate throughout the test. In reality the temperature varies +/- 10 °C during testing (for high temperature testing), and the thermocouple may lose contact with specimen due to vibration.

### 2.3 Experimental characterisation

To establish if the design was successful in achieving controlled impact, a similar characterisation approach to that previously used was conducted to confirm the motion of the arm/hammer relative to the specimen surface being impinged. High speed video footage (120 frames per second (fps), at a resolution of 4k, and in colour) was captured of the apparatus repeatedly striking a specimen at different operating frequencies (i.e. number of impacts per time). Given the reasons for the uncontrolled behaviour previously experienced, two different field of views were considered important; the cam-arm contact, and of the hammer striking the specimen (Figure 5).

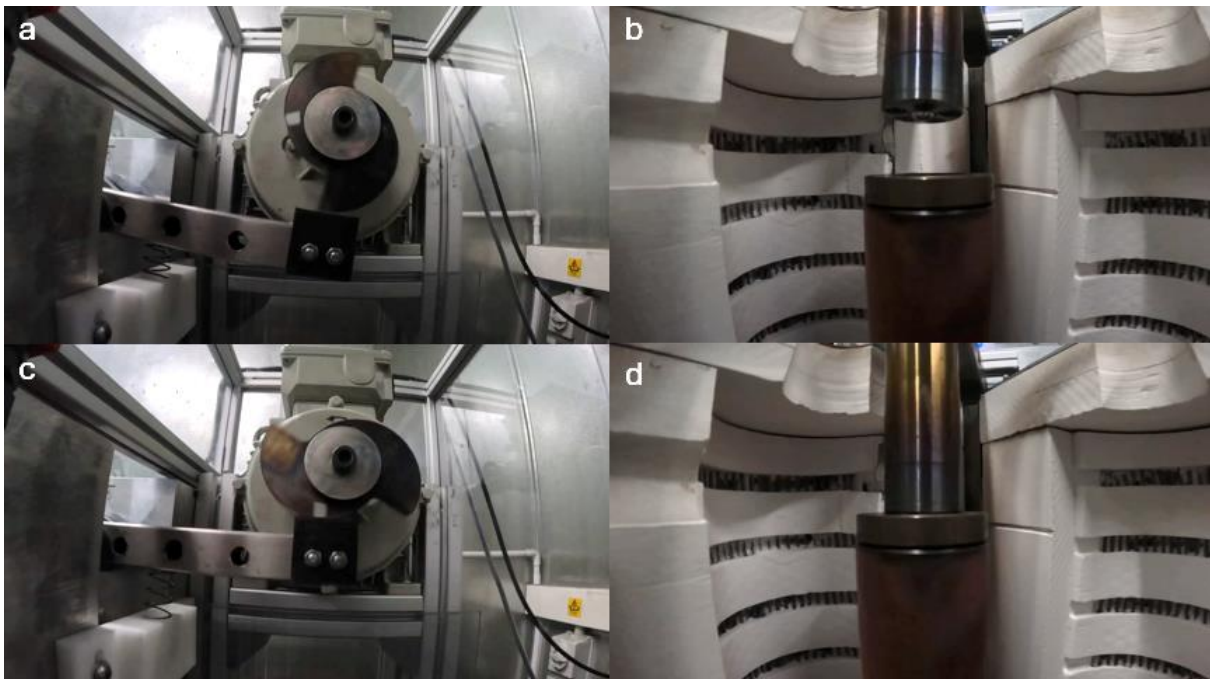


Figure 5 – Frame captures from high-speed video of the apparatus in motion; a) cam shaft rotates to push arm down, b) hammer moves up and spring is loaded, c) cam rotating with arm is lightly-loaded against the cam by the spring, d) hammer impacts sample due to gravitational force and spring unloading.

The captured video was then reviewed to establish if the cam and arm separated at any moment, or if there were any uncontrolled bounces of the striker on the specimen that could cause ‘hidden’ wear. Neither of these were apparent in any of the footage providing strong evidence that the new design has mitigated these problems. It should be noted that the initial intention here was to progress up to capturing video at 1000 fps, as previously used, but as no uncontrolled motion was visible it was deemed unnecessary here.

To further confirm that the impacts are controlled, and only a single impact occurs for every operating cycle of the apparatus, the apparatus was temporarily equipped with a pancake-type load cell to measure the force applied to a specimen at the point of impact. The load cell used was the same device as used previously and is capable of measuring 5-5000 N loads via a data acquisition system sampling at 4.8 kHz. The apparatus was designed in such a way that this load

cell can be swapped in and out of the apparatus easily and with no change to the configuration of the components, thus apparatus motion is the same as when performing regular testing.

The apparatus was operated at a range of frequencies that that generate comparable impact forces to the previous design (and by extension, typically used for testing) and the maximum force recorded for those frequencies is shown in Figure 6. The response in this likely operating region is reasonably linear and comparable to the previous design. The data for a series of single impacts was also examined in detail (Figure 7) and no uncontrolled 'hidden' impacts were recorded by the load cell. The signal decay immediately following each impact is an artefact of the hysteresis of the strain gauge type load cell. The inset of Figure 7 shows the load cell response to a single intended impact on the previous design where the 'hidden' impacts can be seen.

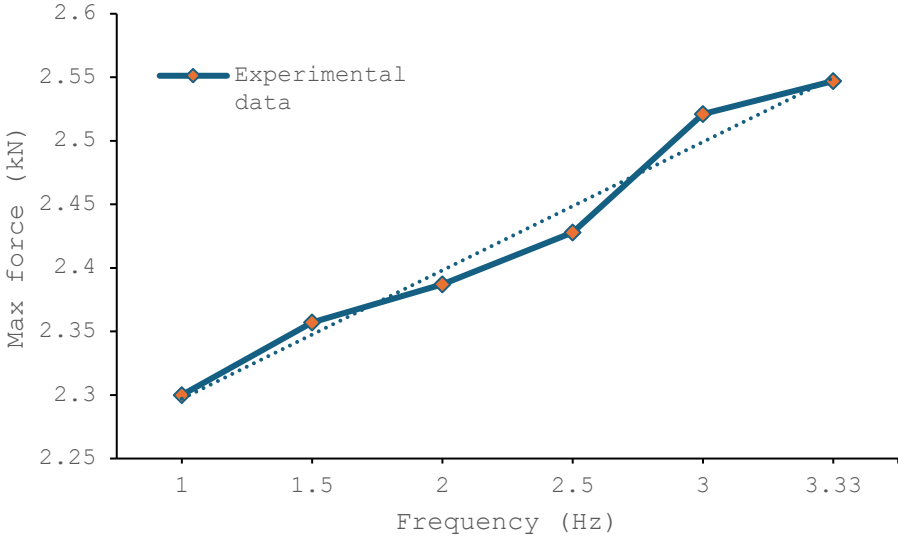


Figure 6 - Measured maximum force at a range of likely operating frequencies (linearity show by dotted line).

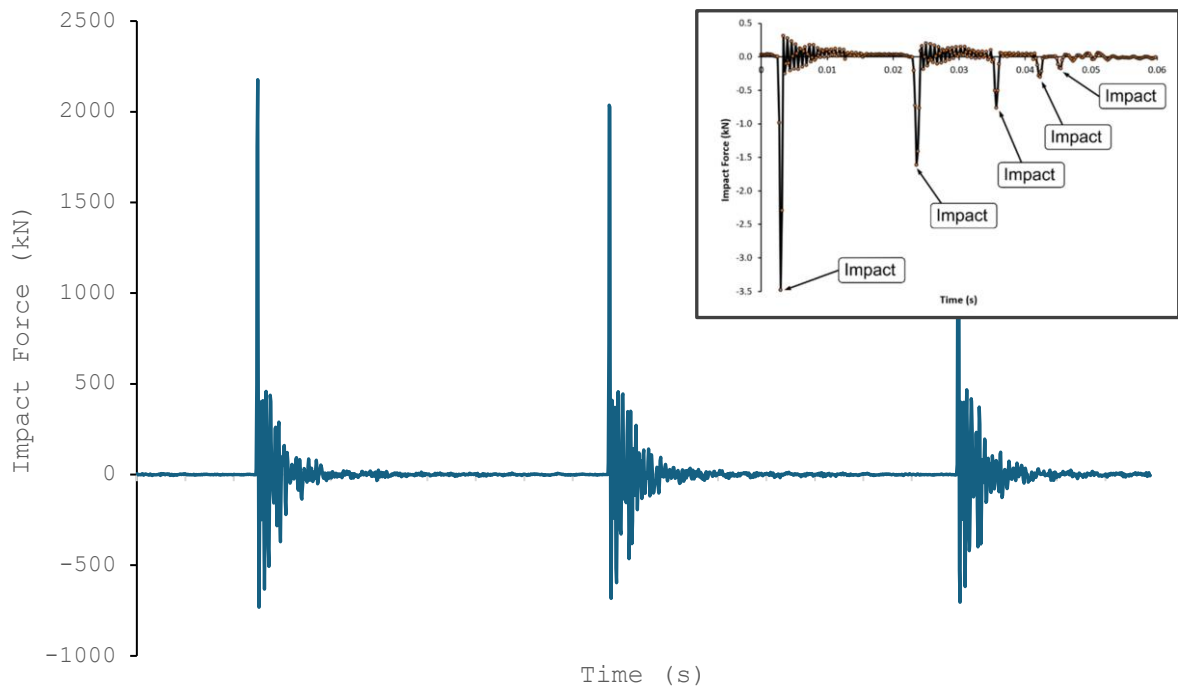


Figure 7- Load cell test results, measured impact force over time for three intended impacts (i.e. three cycles of the apparatus) with (inset) previous apparatus impact force graph for single intended impact (i.e. one cycle of the apparatus), illustrating the extra rebounds [14].

## 2.4 Temperature Analysis

A significant design consideration was that the high operating temperature that the apparatus is capable of when running could reduce the performance, or even damage, of the components, in particular the bearings and motor, the effectiveness thereof being proven via use of a thermographic camera. Thermal images of the rig immediately after operation at 750 °C shows that the bearings and motor remained at relatively low temperatures Figure 8.

The thermographic camera was also used to confirm the capability of the thermocouples to provide adequate temperature information to the control system of the apparatus and thus hold the inside of the heating chamber at the desired temperature. An example of this test is shown in Figure 9.

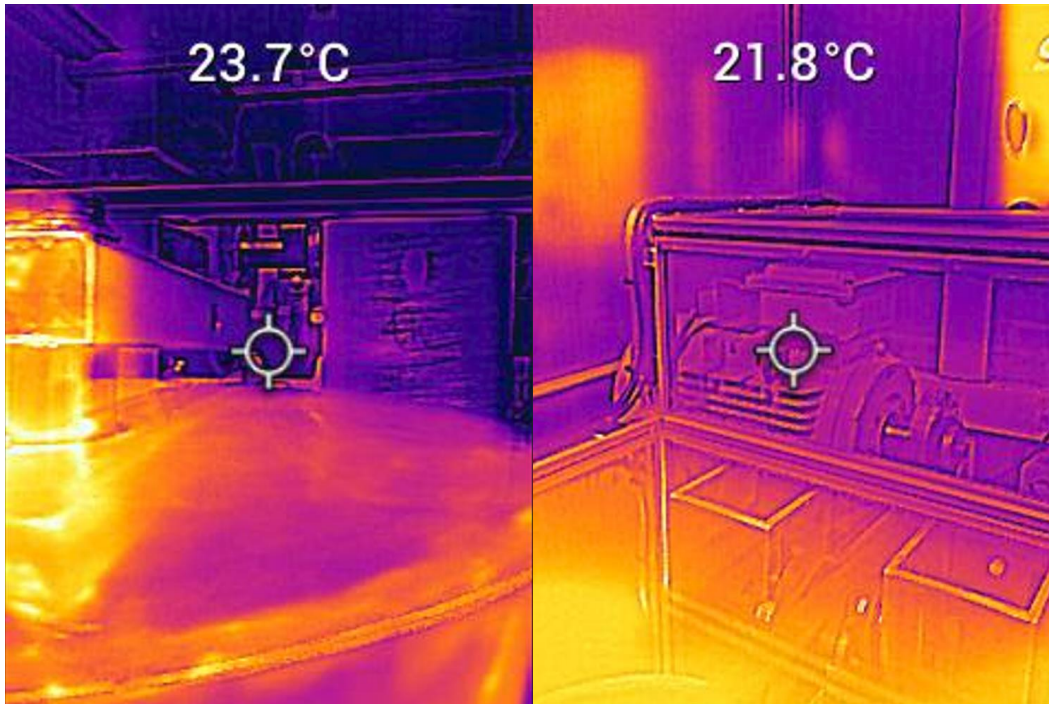


Figure 8 - Thermal image of bearing after 750 °C test, bearing (right), motor (left).

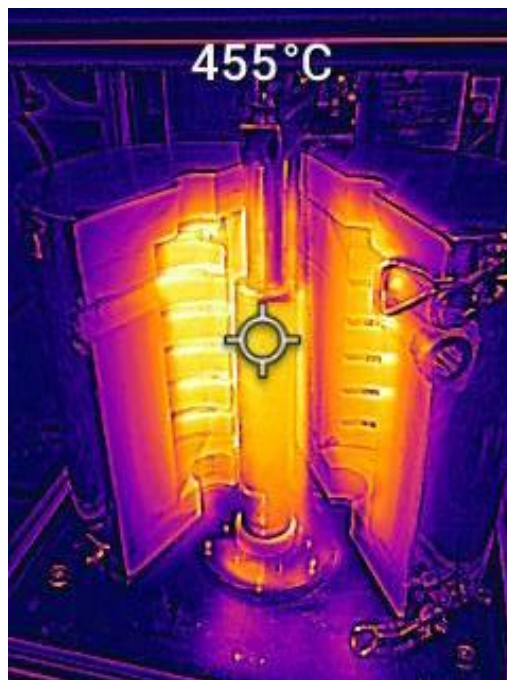
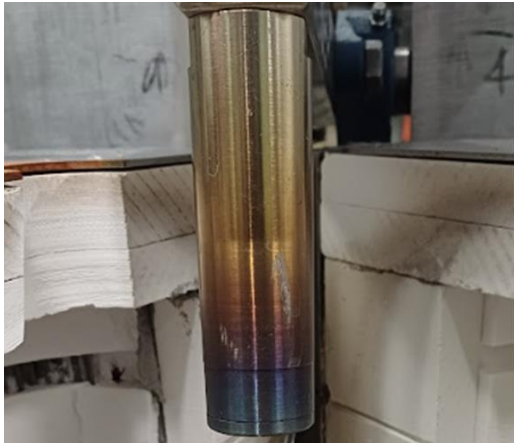


Figure 9 - Thermal image of open furnace after 500 °C test is concluded. Note that a short time passes from the point of apparatus switch-off to being able to open the chamber for safety reasons.

A further check of the temperature capabilities of the apparatus, and to give an indication of the temperature reached by a test specimen, the colour spectrum visible on the surface of the impacting hammer was compared to a tempering chart Figure 10. The colours were also consistently observed on samples used during testing, confirming the temperature control of the apparatus. The sample likely experienced the target temperature as they are adjacent within the chamber.



Color	Temperature
Light Yellow	550 degrees F/290 degrees C
Straw Yellow	640 degrees F/340 degrees C
Yellow	700 degrees F/370 degrees C
Brown	735 degrees F/390 degrees C
Purple Brown	790 degrees F/420 degrees C
Dark Purple	840 degrees F/450 degrees C
Blue	1,000 degrees F/540 degrees C
Dark Blue	1,110 degrees F/600 degrees C

Figure 10 - Thermal gradient visible on impacting hammer after a 750°C testing and corresponding and tempering chart [25].

### **3 Impact wear testing**

Testing designed using Taguchi's full factorial method was used to build an accurate understanding of a material's performance over the full range of temperatures [26]. Five tests were required for each temperature and material to ensure that anomalies were found if they occurred, chosen as it is the smallest possible number of repetitions required to find anomalies [27]. Stainless steel (AISI 304) specimens were tested for five tests at each temperature. Inconel 625 was also tested similarly, albeit with only one test at each temperature, to demonstrate that some metals would experience lower wear rates with higher temperatures. A new striker ball was used for each test.

It was determined that one repetition would be enough to demonstrate that different metals exhibit different behaviour patterns at elevated temperatures. However, one repetition means that the test results are not sufficient to fully characterise the behaviour of Inconel 625 at high temperatures.

Based on the available literature, it was hypothesised that AISI 304 will exhibit more volume loss, higher wear rate and larger deformation around 250 °C, then improve at 500 °C and 750 °C with all high temperature wear rates being higher than the wear rate at room temperature. Inconel 625, however, would be expected to experience decreasing wear rates with increasing temperature.

## **4 Wear scar analysis**

### **4.1 Wear scar morphology**

On completion of each test the striker balls and specimen discs were initially inspected by eye. There was no visible damage or material transfer to the balls, other than some discoloration of those used for the higher temperature tests and witness marks from the ball clamping mechanism. Initial visual inspection of the specimen discs shows a clear trend in those made from AISI 304 where the wear rate decreases as temperature also decreases (Figure 11, from left to right), in contrast with the findings in literature. Samples tested at room temperature, 250 °C and 500 °C all appear perfectly round to the naked eye. The asymmetry in the 750 °C sample was likely caused by the change in metal structure at such a high temperature, as previously found [14].

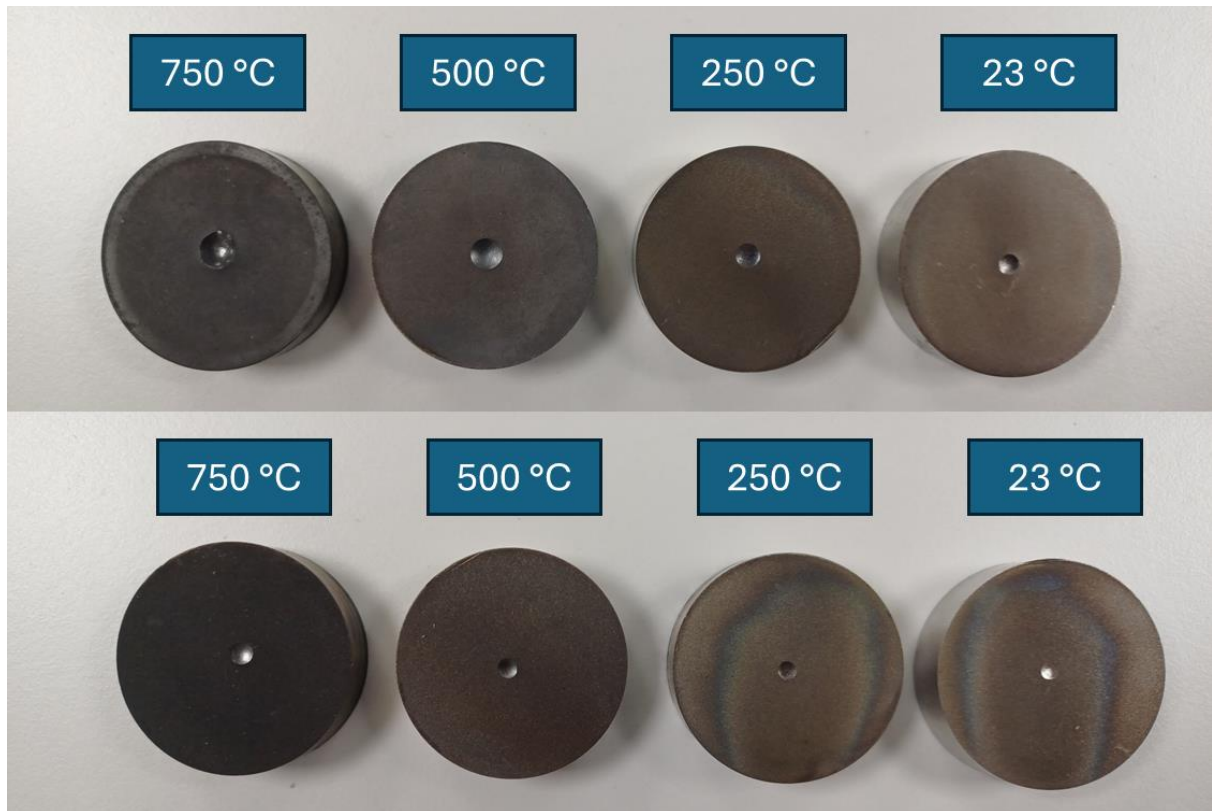


Figure 11 - Typical samples at each temperature tested, AISI 304 stainless steel on top, Inconel 625 on bottom.

Visual inspection of the Inconel 625 samples was much less conclusive than the AISI 304 samples. The wear scars were all roughly of the same size (Figure 11), with the wear scar at 750 °C being slightly larger than the rest. As expected, the Inconel 625 specimens experienced significantly less wear for the same test conditions than the AISI 304.

Figure 12 shows non-contact profilometry (Section 4.2) derived images illustrating the wear scar details. It must be noted that scar size varied significantly between the samples, so for clarity of presentation these images depict the scars at the same size for comparison. The actual diameters are recorded in the figure caption for completeness. As the temperature changes, so do the characteristics of the wear scar and surface. For example, AISI 304 has a clear boundary showing ductile deformation of the material.

The wear scars were typically circular in shape, supporting the ‘small angle’ assumption in Section 2.2, and are similar with the results produced by the previous apparatus. That said there is some ovality (beyond the norm) present in the wear scars produced on the AISI 304 specimens tested at the higher temperatures. This suggests that the temperature driven changes in the material performance may prove the ‘small angle’ assumption to be limited at the higher temperatures. It could be that contact is now ‘compound’ (Figure 1, type C) for these test conditions as the material cannot resist the very small amount of interfacial sliding due to the ‘small angle’, or that magnitude of the wear due what has so far been assumed to be normal impact is such that the ‘small angle’ becomes two large (or both) as the arc length increases.



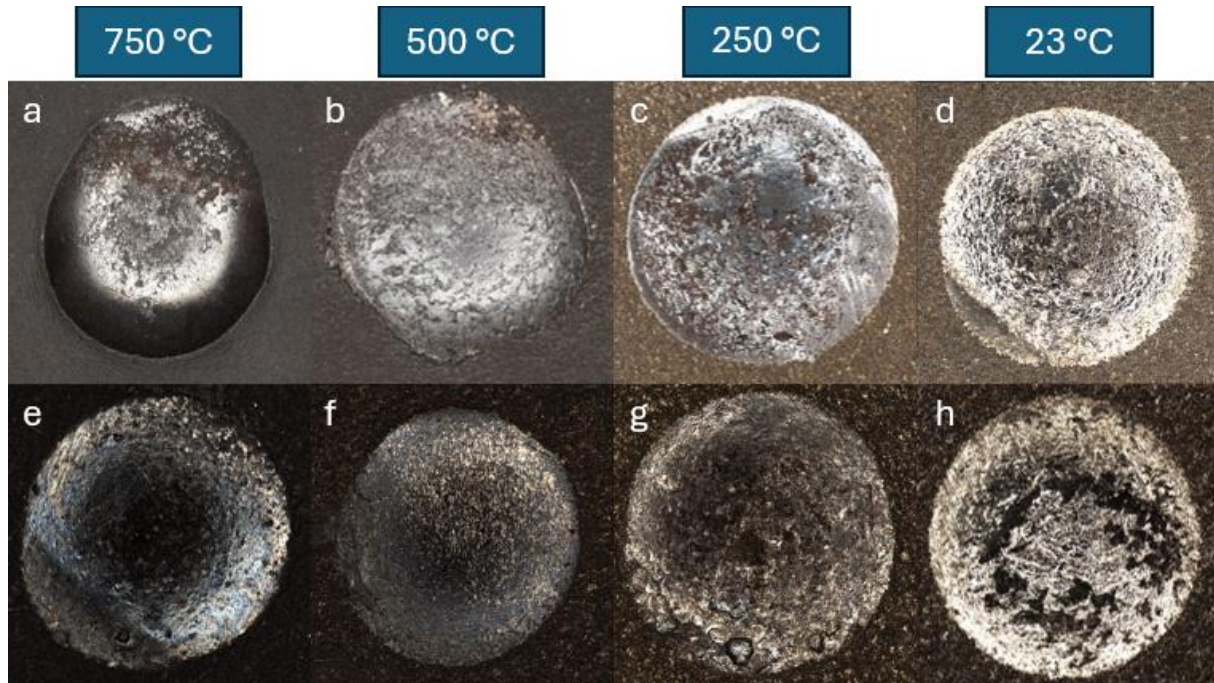


Figure 12 - Wear scar close-up images top row AISI 304, bottom row Inconel 625. Wear scar diameters: a) 5.64 mm, b) 4.79 mm, c) 3.75 mm, d) 3.09 mm, e) 3.24 mm, f) 3.02 mm, g) 2.84 mm, and h) 2.52 mm

#### 4.2 Wear scar geometry

Each of the samples tested at each condition were measured using the same methodology as previous studies by the authors of this analysis [14] where 3D non-contact profilometry (focus variation type, Bruker Alicona SL) is used to scan each wear scar and enough of the surrounding ground flat specimen surface to form a consistent reference in the z-plane, thus removing any need for post-processing (levelling or similar) to achieve the same. This enables direct volume calculation both above and below the reference surface using software (MeasureSuite v.5.3.9). The average volume loss is calculated and used to plot wear volume versus temperature for each material (Figures 13 & 14).

The AISI 304 specimens experienced a consistent and significant increase in wear scar size at each temperature, while Inconel shows a much less linear behaviour. The Inconel 625 specimens exhibit a smaller rate of increase, and the depth of the wear scar begins to reduce at the highest temperature (Figure 15).

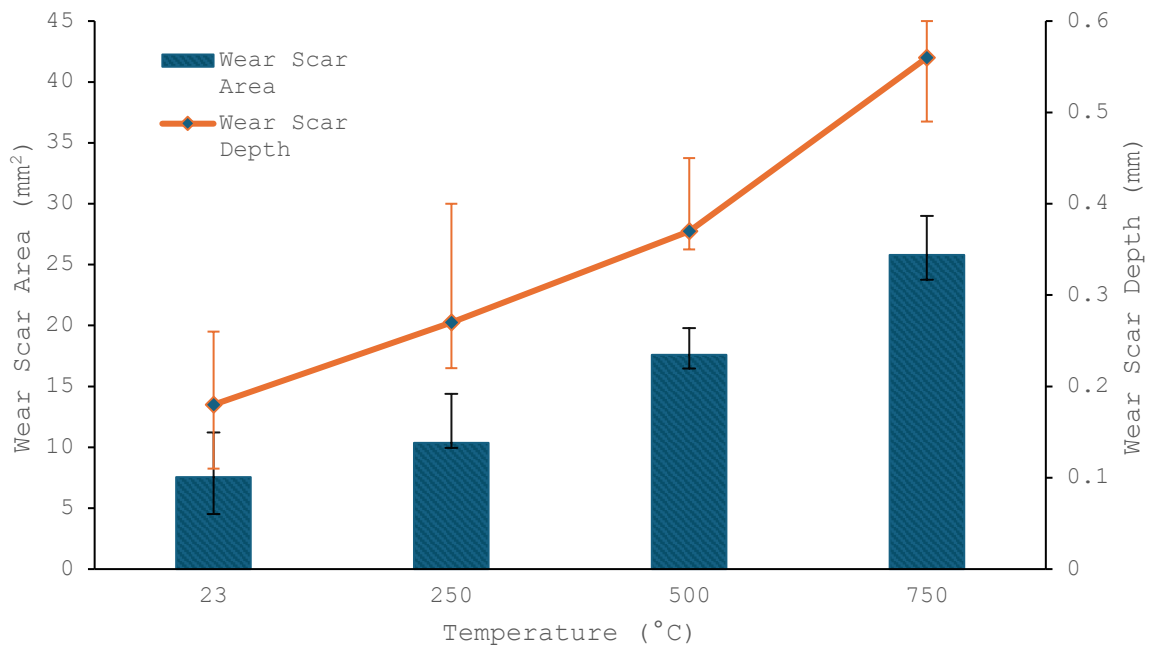


Figure 13 - Wear scar area and depth results for AISI 304.

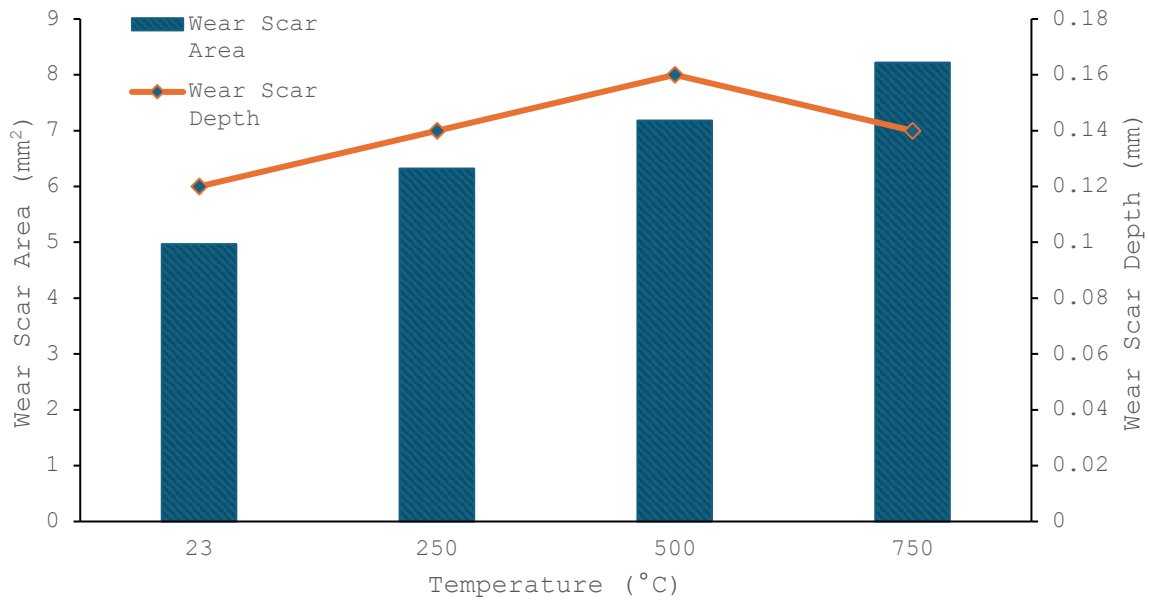


Figure 14 - Wear scar area and depth results for Inconel 625.

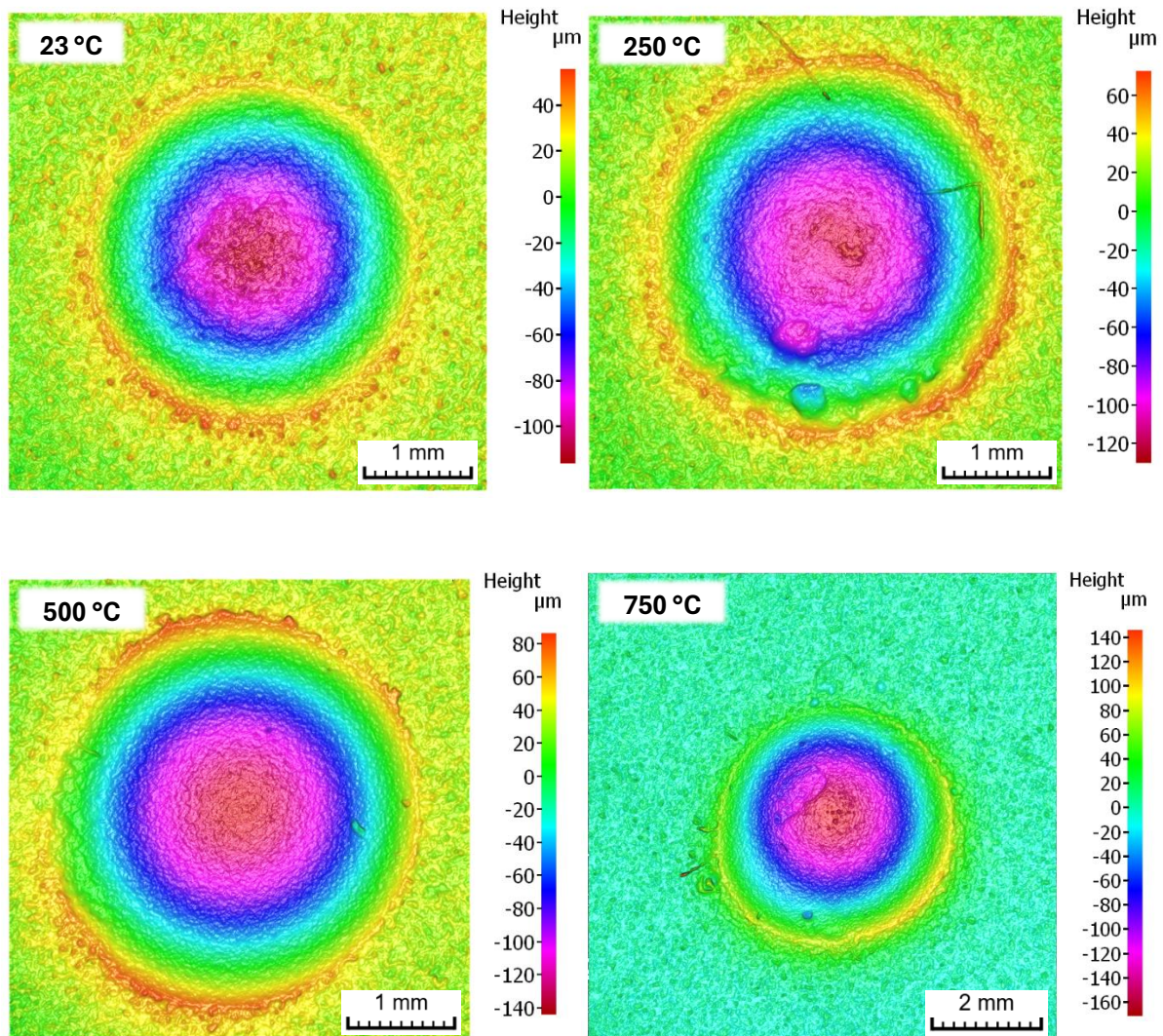


Figure 15 – Typical depth contours for Inconel 625 (note the different x-y plane scale for 750 °C, and different z- scale for all).

### 4.3 Wear scar volume

The non-contact profilometry data was also used to calculate wear volume loss, again using the methodology previously established by Slatter et al [14]. The dataset can be used to find the volume of material above and below the nominal surface of the sample. As established previously, simply using the data representing the volume below the surface is not sufficient to find the volume loss as it does not account for the volume that was displaced, usually as ductile shoulders around the wear scar edge, away from the contact zone from the impacts. It is therefore important to calculate the ratio of volume above and below the surface to characterise the wear scar, and understand how much of the material gets removed and how much gets displaced. This is particularly important for testing at elevated temperatures, or indeed varying temperature in general, as the ductility of the material being investigated may change.

Table 1 shows the mean wear values for the AISI 304 samples. There is a significant increase in wear rate with increasing temperatures. This is clearly seen as the volume loss increases by 97%

between room temperature and 250 °C, and further increases by 94% between 250 °C and 500 °C. The volume loss increases by 26% between 500 °C and 750 °C. This may give a false indication that the wear did not significantly increase between those temperatures, however the displaced volume above the surface increases by 572% and volume below the surface increases by 84%. These show that the wear rate significantly increased between 500 °C and 750 °C and reinforces the conclusion of Slatter et al. regarding the importance of selecting the appropriate measurement method [14].

Table 1 - Average volume results for AISI 304

Temperature (°C)	Volume above (mm <sup>3</sup> )	Volume below (mm <sup>3</sup> )	Volume ratio	Volume loss (mm <sup>3</sup> )
RT	0.03	0.74	24:1	0.71
250	0.08	1.48	19:1	1.40
500	0.32	3.03	9:1	2.71
750	2.15	5.56	3:1	3.41

The volume ratio can also be analysed. The ratio initially increases at 250 °C then quickly decreases at 500 °C and 750 °C. This trend was clear when creating wear scar depth contour plots Figure 16. It should be noted that the room temperature wear scar appears larger in this figure than the others included to more easily distinguish the contours. The images show that the very top of the wear scar features (i.e. the shoulders) moves further above the plane of surface with higher temperatures. This can be explained by considering the properties of AISI 304 at elevated temperatures, becoming slightly more brittle around 250 °C, then increasing in ductility at 500 °C and 750 °C. The metal is therefore displaced rather than removed, as it undergoes plastic flow instead of brittle fracture.

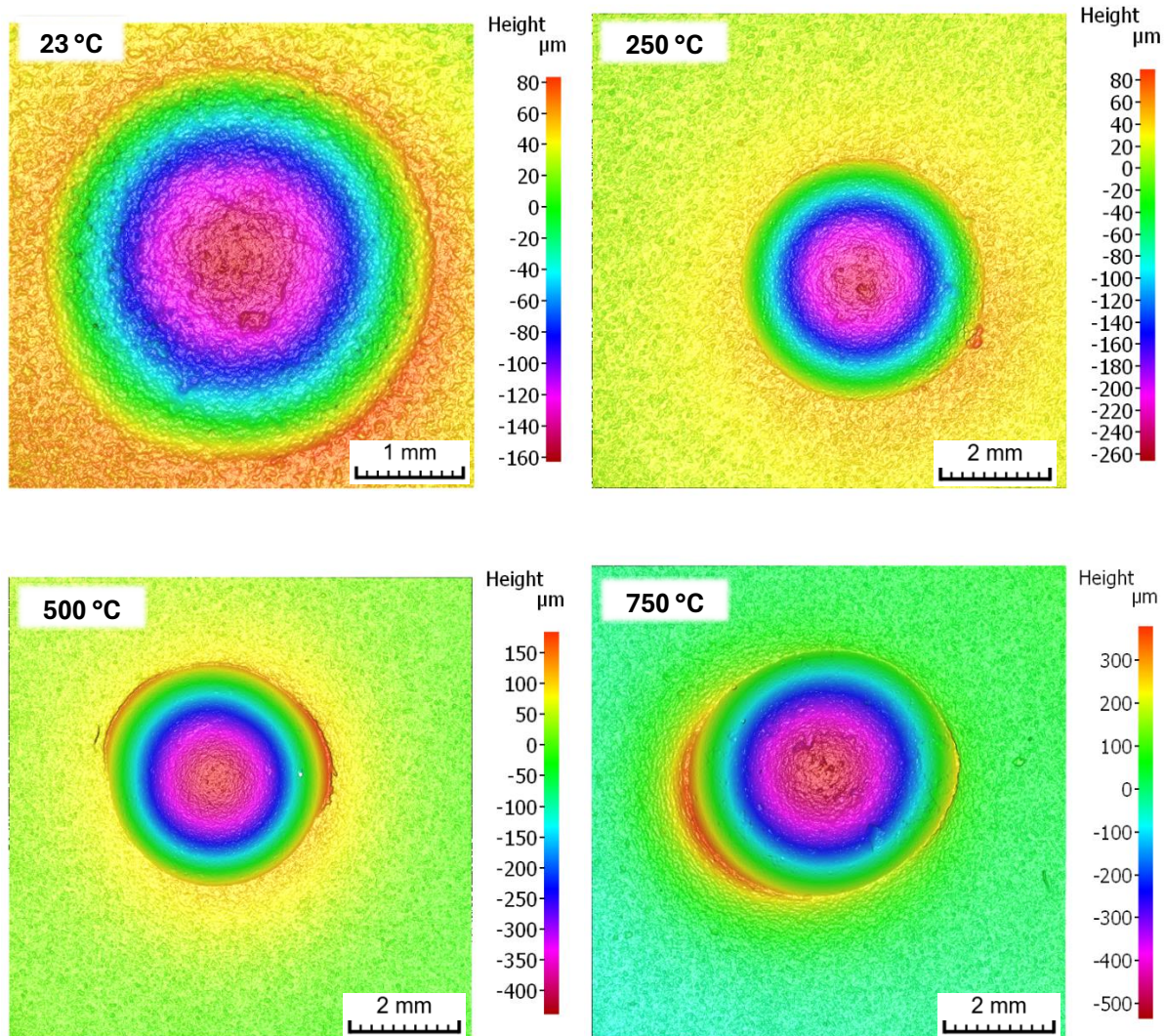


Figure 16 - Typical sample depth contour plots for AISI 304 (note the different x-y plane scale for 23 °C, and different z- scale for all).

Volume loss results for Inconel were also obtained similarly. As previously noted (Section 3), only one repetition was completed at each temperature for Inconel 625 meaning that the results offer less confidence. Table 2 shows the volume results for Inconel 625. The wear volume increases by 25% between room temperature and 250 °C, then 57% from 250 °C to 500 °C, then it decreases by 43% between 500 °C and 750 °C. The percentage change in wear volume is smaller for Inconel 625 than it is for AISI 304. The most significant change in wear performance compared to AISI 304 is that the wear volume at 750 °C exhibited lower wear volume than 250 °C and 500 °C. The wear volume was also similar to that of Inconel 625 tested at room temperature. This clearly shows that Inconel 625 behaves differently to AISI 304, both in wear magnitude and trend, and that this new apparatus can distinguish between different materials, at different temperatures successfully.

Table 2 - Wear scar volume measurement results for Inconel 625.

Temperature (°C)	Volume above (mm <sup>3</sup> )	Volume below (mm <sup>3</sup> )	Volume ratio	Volume loss (mm <sup>3</sup> )
RT	0.026	0.266	10:1	0.24
250	0.059	0.36	6:1	0.301
500	0.039	0.513	13:1	0.474
750	0.261	0.53	2:1	0.269

Figure 17 shows the relationship between wear volume and temperature for both Inconel 625 and 304 stainless steel. This shows that volume loss for Inconel 625 is much lower and does not follow the same uniform pattern as AISI 304.

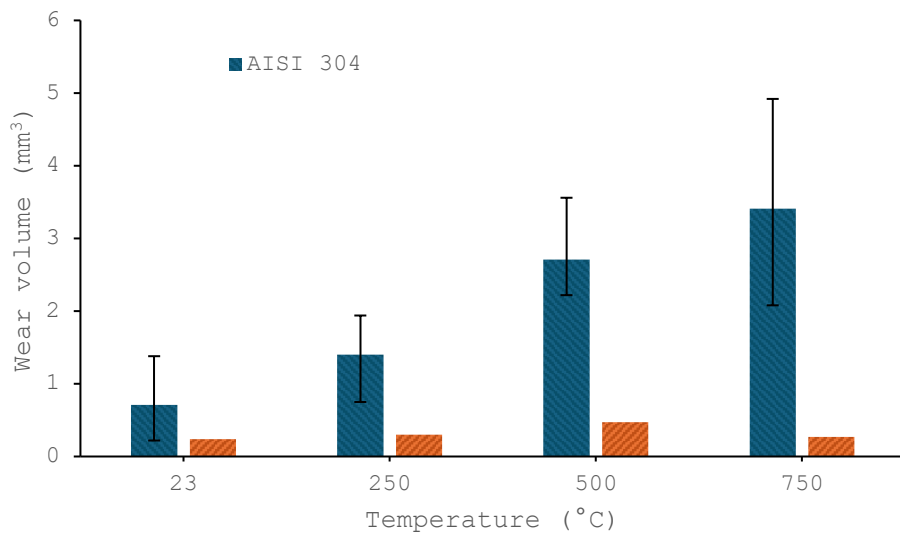


Figure 17 - Volume loss graph for both materials tested; AISI 304 (blue, mean of 5 tests, error bars represent maximum and minimum measured values) and Inconel 625 (orange, single tests).

There was a clear correlation between temperature and wear for AISI 304, as expected, however repeated tests at the same conditions gave results with a relatively large error. Table 3 shows the largest and smallest differences at each temperature. It is interesting to note that these are more significant than those previously presented [14], even though the apparatus used for those tests is less controlled dynamically, suggesting that the effect of temperature (and perhaps more importantly the control thereof) is more important to the impact wear resistance of these types of metals.

That said, although there were differences between repetitions for the same temperature, the general trend of increased wear at higher temperatures was mostly maintained throughout. For example, at no point did the largest wear scar depth at 250 °C become larger than the smallest wear depth at 500 °C. The main exception for this was wear volume between 500 °C and 750 °C and as discussed in Section 4.3. This led to some tests at 500 °C having higher wear volume than some tests at of 750 °C, but the mean for 750 °C is still higher than for 500 °C.

Table 3 - Percentage differences of wear scar properties for AISI 304 stainless steel specimens

Temperature (°C)	Volume (%)	Area (%)	Depth (%)
Largest difference (%)			
RT	498.3	148.1	136.4
250	133.0	42.9	81.8
500	41.0	17.7	12.1
750	73.1	22.1	22.5
Smallest difference (%)			
RT	16.3	11.0	0.0
250	5.0	3.3	3.7
500	0.0	2.1	0.0
750	3.7	2.2	0.0

## 5 Discussion & Reflections

Testing was able to demonstrate that the apparatus design was robust and reliably capable of providing impact wear testing in a more controlled manner than previously achieved and up to a temperature of 750°C. Operation of this new design at temperatures higher than this is not recommended due to the likely degradation in performance of the components selected. The specification of the heating modules is such that the operating temperature could be higher (estimated to be 950-1000 °C) but this would necessitate careful selection of the materials used for the specimen holder, hammer and hammer arm. At these elevated temperatures it is difficult to combine the thermal, mechanical, and manufacturability properties required into one type of material.

As discussed in Section 1, impact wear apparatus often needs careful consideration of its dynamics to provide consistent repetitive impacts upon the specimen surface. The new design has good linearity of response for its likely operating range. The sizing and geometry (e.g. length of hammer arm, effective mass of arm-striker system) of the new apparatus means that it cannot produce lower loads that have been possible before, but this is an acceptable trade-off for the thermal mitigations. The apparatus was also operated at increasing speeds and above approximately 3.5 Hz the apparatus became increasingly uncontrolled and produced much lower impact forces due to the changed interaction of the cam-arm-striker system.

For high temperature work, excellent control of temperature is also critical. The general thermal response of the apparatus should also be taken into account when conducting testing to consider any residual heat recent earlier testing and thermocouples should be used outside of the heating chamber to ensure consistency (and, indeed user safety). In the data presented here, the variability in the room temperature testing may be in part as a result of this, even though the thermocouples installed in the apparatus were reporting the temperature to be around 23 °C.

Due consideration should also be taken by those testing with this type of apparatus on the performance of the materials selected, even for miscellaneous components such as the screws used to retain specimens and strikers that may degrade at high temperatures. During the testing carried out to assess the new apparatus design described here, it became apparent that temperature and vibration combined accelerated the failure of components.

The initial testing conducted for purposes of judging the efficacy of the design has confirmed that AISI 304 experiences a steadily increasing wear scar size with increasing temperature, in contrast to the literature. It also indicates that Inconel 625 has a non-linear response to wear, with wear reducing when temperature further raised beyond those used in the literature.

Given the nature of this study was to only in part conduct ‘learning tests’, the variation in wear is important to note for those designing a much more comprehensive Design of Experiment using apparatus such as this. It is suggested therefore that for impact testing at elevated temperatures it is particularly important to consider completing more test repetitions than are typically found in the literature for equivalent tests at room temperature given the potential for non-linearity in response as temperature changes induce change in material properties.

## 6 Conclusion

It is hoped that the commentary and reflections offered on the development of this new apparatus and initial testing provide researchers with an initial approach to high temperature repetitive impact testing. Formally, the following concluding statements can be made for this work:

1. The new design of apparatus has shown to be reliably capable of repetitive impact wear testing;
  - a. up to 750 °C, significantly exceeding previously reported designs.
  - b. with more controlled repetitive impacts than previously evidenced.
2. Wear behaviour was characterised for AISI 304 stainless steel, with steadily increasing wear with increasing temperature. This contrasts with the, albeit limited, literature which reports a non-linear response.
3. An indication of the wear behaviour for Inconel 625 was established, with a non-linear level of wear, with the wear scar beginning to become smaller at the highest temperature.

## 7 Acknowledgements

The authors wish to acknowledge the technical contribution of: Dr Richard Wellman, Harry Buxton, and the other undergraduates and graduates whose project work inspired the design of this apparatus. The authors also acknowledge Rolls Royce plc. for their support of impact wear studies at The University of Sheffield.

## 8 References

- [1] P. A. Engel, ‘Percussive impact wear: A study of repetitively impacting solid components in engineering’, *Tribology International*, vol. 11, no. 3, pp. 169–176, Jun. 1978, doi: 10.1016/0301-679X(78)90002-6.
- [2] J. R. Laguna-Camacho *et al.*, ‘A study of the wear damage on gas turbine blades’, *Engineering Failure Analysis*, vol. 61, pp. 88–99, Mar. 2016, doi: 10.1016/j.engfailanal.2015.10.002.
- [3] Q. M. Mehran, M. A. Fazal, A. R. Bushroa, and S. Rubaiee, ‘A Critical Review on Physical Vapor Deposition Coatings Applied on Different Engine Components’, *Critical Reviews in Solid State and Materials Sciences*, vol. 43, no. 2, pp. 158–175, Mar. 2018, doi: 10.1080/10408436.2017.1320648.



- [4] Z. Shi, X. Li, N. Duan, and Q. Yang, 'Evaluation of tool wear and cutting performance considering effects of dynamic nodes movement based on FEM simulation', *Chinese Journal of Aeronautics*, vol. 34, no. 4, pp. 140–152, Apr. 2021, doi: 10.1016/j.cja.2020.08.003.
- [5] Z. Dong, F. Jiang, Y. Tan, F. Wang, R. Ma, and J. Liu, 'Review of the Modeling Methods of Bucket Tooth Wear for Construction Machinery', *Lubricants*, vol. 11, no. 6, Art. no. 6, Jun. 2023, doi: 10.3390/lubricants11060253.
- [6] R. Fricke, 'The repetitive impact wear of steels for hydro-powered mining machinery', 1991, Accessed: May 06, 2024. [Online]. Available: <http://hdl.handle.net/11427/18214>
- [7] 'Factors affecting wear and galling – British Stainless Steel Association'. Accessed: Dec. 10, 2023. [Online]. Available: [https://bssa.org.uk/bssa\\_articles/factors-affecting-wear-and-galling/](https://bssa.org.uk/bssa_articles/factors-affecting-wear-and-galling/)
- [8] V. Gopi, R. Sellamuthu, and S. Arul, 'Measurement of Hardness, Wear Rate and Coefficient of Friction of Surface Refined Al-Cu Alloy', *Procedia Engineering*, vol. 97, pp. 1355–1360, Jan. 2014, doi: 10.1016/j.proeng.2014.12.416.
- [9] M. Zalzal, R. Lewis, and T. Slatter, 'A new predictive model for normal and compound impact wear', *Wear*, vol. 480–481, p. 203954, Sep. 2021, doi: 10.1016/j.wear.2021.203954.
- [10] 'Gas turbine operating parameters?', Thunder Said Energy. Accessed: Apr. 17, 2024. [Online]. Available: <https://thundersaidenergy.com/downloads/gas-turbines-operating-parameters/>
- [11] 'Gas Turbine Efficiency - An Overview', Allied Power Group. Accessed: May 15, 2024. [Online]. Available: <https://alliedpg.com/latest-articles/gas-turbine-efficiency/>
- [12] H. A. Sherif and F. A. Almufadi, 'Analysis of elastic and plastic impact models', *Wear*, vol. 412–413, pp. 127–135, Oct. 2018, doi: 10.1016/j.wear.2018.07.013.
- [13] R. Lewis, 'A modelling technique for predicting compound impact wear', *Wear*, vol. 262, no. 11, pp. 1516–1521, May 2007, doi: 10.1016/j.wear.2007.01.032.
- [14] T. Slatter, M. Zalzal, and R. Lewis, 'Analysis of reciprocating hammer type impact wear apparatus', *Wear*, vol. 523, p. 204816, Jun. 2023, doi: 10.1016/j.wear.2023.204816.
- [15] X. Chen, L. Wang, L. Yang, R. Tang, Y. Yu, and Z. Cai, 'Investigation on the impact wear behavior of 2.25Cr–1Mo steel at elevated temperature', *Wear*, vol. 476, p. 203740, Jul. 2021, doi: 10.1016/j.wear.2021.203740.
- [16] T. Ootani, N. Yahata, A. Fujiki, and A. Ehira, 'Impact wear characteristics of engine valve and valve seat insert materials at high temperature (impact wear tests of austenitic heat-resistant steel SUH36 against Fe-base sintered alloy using plane specimens)', *Wear*, vol. 188, no. 1, pp. 175–184, Sep. 1995, doi: 10.1016/0043-1648(95)06656-X.
- [17] M. Varga, H. Winkelmann, and E. Badisch, 'Impact of microstructure on high temperature wear resistance', *Procedia Engineering*, vol. 10, pp. 1291–1296, Jan. 2011, doi: 10.1016/j.proeng.2011.04.215.
- [18] S. Hernandez, 'High Temperature Wear Processes'. 2014. Accessed: Oct. 01, 2023. [Online]. Available: <https://www.diva-portal.org/smash/get/diva2:989814/FULLTEXT01.pdf>

- [19] D. Kesavan and M. Kamaraj, 'The microstructure and high temperature wear performance of a nickel base hardfaced coating', *Surface and Coatings Technology*, vol. 204, no. 24, pp. 4034–4043, Sep. 2010, doi: 10.1016/j.surfcoat.2010.05.022.
- [20] Y. Zhou, R. Wang, J. Hu, and X. Lei, 'High-temperature wear mechanism of roller cone bit spiral seal', *Wear*, vol. 532–533, p. 205112, Nov. 2023, doi: 10.1016/j.wear.2023.205112.
- [21] '- William Rowland'. Accessed: Mar. 14, 2024. [Online]. Available: <https://www.william-rowland.com/news/item/how-does-heatits-properties>
- [22] G. Rajaram, S. Kumaran, and T. S. Rao, 'High temperature tensile and wear behaviour of aluminum silicon alloy', *Materials Science and Engineering: A*, vol. 528, no. 1, pp. 247–253, Nov. 2010, doi: 10.1016/j.msea.2010.09.020.
- [23] S. Narayan and A. Rajeshkannan, 'Hardness, tensile and impact behaviour of hot forged aluminium metal matrix composites', *Journal of Materials Research and Technology*, vol. 6, no. 3, pp. 213–219, Jul. 2017, doi: 10.1016/j.jmrt.2016.09.006.
- [24] A. S. Khanna, 'Fundamentals of High Temperature Oxidation/Corrosion', in *High Temperature Corrosion*, WORLD SCIENTIFIC, 2015, pp. 1–31. doi: 10.1142/9789814675239\_0001.
- [25] 'All you need to know about the heat-affected zone'. Accessed: May 02, 2024. [Online]. Available: <https://www.thefabricator.com/thefabricator/article/shopmanagement/all-you-need-to-know-about-the-heat-affected-zone>
- [26] J. Antony, '6 - Full factorial designs', in *Design of Experiments for Engineers and Scientists (Third Edition)*, J. Antony, Ed., Elsevier, 2023, pp. 65–87. doi: 10.1016/B978-0-443-15173-6.00009-3.
- [27] E. Eypasch, R. Lefering, C. K. Kum, and H. Troidl, 'Probability of adverse events that have not yet occurred: a statistical reminder', *BMJ*, vol. 311, no. 7005, pp. 619–620, Sep. 1995, doi: 10.1136/bmj.311.7005.619.